

Research article

Mitosis targeting in non-small lung cancer cells by inhibition of PAD4

Xiangmei Wu^{a,d}, Liujia Chan^{b,c}, Di Zhu^c, Yuheng Pang^b, Mulan Jin^{a,**}, Yuji Wang^{c,***}, Wenjing Wang^{b,*}

^a Department of Pathology, Beijing ChaoYang Hospital, Capital Medical University, Beijing, 150086, China

^b Beijing Institute of Hepatology, Beijing YouAn Hospital, Capital Medical University, Beijing, 100069, China

^c Department of Medicinal Chemistry, College of Pharmaceutical Sciences, Capital Medical University, Beijing, 100069, China

^d Department of Pathology, Beijing Geriatric Hospital, Beijing, 100095, China

ARTICLE INFO

Keywords:

Lung carcinoma
PAD4
Mitosis arrest

ABSTRACT

PAD4 expression and activity were significantly up-regulated in lung cancer tissues suggesting that PAD4 could be a possible target for lung cancer treatment. In this study we had demonstrated that PAD4 expression was higher in lung cancer patients whom with lymphnode metastasis and pleural invasion. Inhibiting PAD4 with a small molecular inhibitor could induce apoptosis and suppress growth in lung cancer cells. We used RNA-sequencing to further investigate transcriptional changes that induced by PAD4 inhibition, and results suggested its affected mostly on the cell cycle, mitotic cell cycle process, p53 signaling pathway. By using image flow cytometry analysis, we found that PAD4 inhibited by YW3-56 could accumulate cells in the G1/G0 phases and reducing the fraction of G2/M and S phase cells. Quantification of different phase of mitosis in cells treated with YW3-56 revealed an increasing trend of telophase and prophase cells. Taken together, our data indicated that PAD4 inhibitor could affect cell cycle and mitosis of lung cancer cells, and targeting PAD4 could be a promising strategy for discovery novel anti-NSCLC treatments.

1. Introduction

Lung cancer is one of the most important malignant tumors that affect human health and life. According to the statistics in 2020, the incidence of lung cancer is 11.4% and it remained the leading cause of cancer death in the world [1]. Non-small cell lung cancer (NSCLC) which mainly includes adenocarcinomas and squamous cell carcinomas account for about 80% of all lung cancers. Adenocarcinoma has become the most common histological sub-type of primary lung cancer [2]. Lung adenocarcinoma patients lack specific clinical symptoms in the early stage, local invasion or distant transformation often occur in advanced lung cancer patients and the treatment effect is usually poor. Although targeted therapy and immunotherapy have achieved notable clinical efficacy, the clinical beneficiaries are still very limited and the 5-year overall survival rate is less than 20% [3–5]. Furthermore, due to the genetic heterogeneity of cancer, single targeted therapies are often not successful [6]. Therefore, it is necessary to explore more effective

* Corresponding author.

** Corresponding author.

*** Corresponding author.

E-mail addresses: kinmokuran@163.com (M. Jin), wangyuji@ccmu.edu.cn (Y. Wang), wangwenjing85321@ccmu.edu.cn (W. Wang).

molecular targets for non-small cell lung cancer treatment.

Peptidyl arginine deiminases (PADs) are the family of Ca^{2+} -dependent post-translational modification enzymes which catalyze the conversion of arginine residues to non-coded citrulline residues, and this reaction is referred to as citrullination or deimination [7]. PAD-mediated citrullination alters the molecular conformation and biological activity of proteins. PAD4, which was initially cloned from human myeloid leukemia HL-60 cells, is mainly expressed in monocytes, eosinophils, lymphocytes and neutrophils. It is the only type of PAD that can enter into the nucleus with a classic nuclear localization sequence (NLS) [8,9].

Previous studies have confirmed that PAD4 is significantly associated with pathogenesis and susceptibility of rheumatoid arthritis (RA) [10]. In recent years, accumulated evidences have demonstrated that PAD4 is highly expressed in a variety of malignant tumors including non-small cell lung cancers and it plays a vital role in the process of tumorigenesis [11,12]. However, there were also few reports that reveal the relationship between the expression of PAD4 and relevant clinicopathological features and the specific molecular mechanism of PAD4 in non-small cell lung cancer. Liu et al. found that PAD4 was overexpressed in A549 lung cancer cells and PAD4-mediated EMT transition could be a novel epigenetic mechanism in non-small lung cancer cells [13].

In this study, we investigated the expression of PAD4 in lung cancer tissues and further explored the underlying mechanism of PAD4 in tumorigenesis in non-small lung cancer cell lines.

2. Materials and methods

2.1. Patients and tissue specimens

Tissue specimens were obtained from 63 lung adenocarcinoma patients who underwent complete resection in Beijing Chao-Yang Hospital, Capital Medical University from March 2014 to December 2018. All patients were not treated with radio or chemical therapy before operation. The age of the patients ranged from 35 to 77 years (median age, 56 years). The degree of tumor differentiation was judged according to World Health Organization standard. Tumor size, nodal metastasis and other clinical information were obtained from medical records and the pathology reports. Informed consent was obtained from all enrolled patients, and all procedures and protocols were approved by the institutional ethics committee of Beijing Geriatric Hospital (BJLNYY-ER-2020-005).

2.2. Immunohistochemical examination

All of tissue paraffin blocks were cut into 4 μm thick tissue sections. After conventional dewaxing and rehydration, the sections were placed in EDTA buffer (pH 8.0), and heated to 95 °C for 30 min for antigen repair. Endogenous peroxidase activity was blocked by incubation of slices in 3% H_2O_2 for 20 min at room temperature. And then all samples were incubated with primary antibodies against PAD4 (1:100; Novus Biologicals) overnight at 4 °C and a homologous secondary antibody for 30 min at room temperature in a wet box. Then the slides were stained with freshly dispensed DAB (diaminobenzidine solution) and observed under a microscope. At last, all the sections were counterstained with hematoxylin, dehydrated, airdried, and mounted. In this process, the slides were all washed three times in PBS (phosphate buffer solution, pH 7.3) for 5 min each time before each step. PBS instead of primary antibody was applied for negative controls.

Interpretation of data: PAD4 positive staining was revealed as brown yellow or brown granules in the nucleus and cytoplasm, 5 HPF fields were selected in the high expression area. Both the cell staining intensity and the percentage of positive cells in the section were counted: $\leq 10\%$ cells showed different degrees of staining was judged as + (weak positive); 10%–30% cells show strong staining or $\leq 70\%$ cells show weak or medium staining was judged as ++ (positive); $> 30\%$ cells show strong staining or $> 70\%$ cells show medium staining was judged as +++ (strong positive). Weak positive and positive were regarded as PAD4 low-expression group, and strong positive was regarded as PAD4 high-expression group. All the slides were screened by two pathologists independently.

2.3. Reagents and cell lines

The compound YW3-56 (with purity $> 95\%$) was synthesized in Yuji Wang's lab from Capital Medical University as reported before [14]. Annexin V-FITC staining Apoptosis Detection Kit (BD Biosciences Pharmingen, San Diego, CA, USA) was used to detect apoptotic cell death. Cell Counting Kit-8 and Cell Cycle detection kit (AbMole Bioscience, Houston, TX, USA, USA) was used to evaluate cells viability and cell cycle distribution of lung cancer cells that treated by YW3-56. A549 cells and 95D cells was obtained from Capital Medical University, and STR detection was performed before used in this study.

2.4. Cell viability assay

A549 and 95D cells viability that treated with different concentration of YW3-56 (0, 2.5, 5, 10, 15, 20, 40 μM) for 48 h was detected by CCK-8 assay. In brief, cells were seeded at a density of 4×10^3 per well in 96-well plates and cultured over-night before treated with different concentration of YW3-56, the same concentration of DMSO in medium was used as control. After 48 h culturing, 10 μL CCK-8 reagent was added and cultured for additional 2 h. The plates were then measured at 450 nm using Full wavelength microplate reader (Mutiskan GO, USA). Cell viability was analyzed as reported before [15].

2.5. Flow cytometry detection of apoptosis

Annexin V-FITC apoptosis kit was used to investigate apoptosis in A549 and 95D cells induced by YW3-56 according to the manufacturer's instructions. In brief, 95D and A549 cells were seeded at 1×10^5 cells per well in 6-well plate for 12 h before exposed to YW3-56 (with final concentration of 0, 5, 10, 15 μM) for 48 hr. Cells were then collected, washed triple times with ice-cold PBS, and resuspended in 100 μL of binding buffer followed by adding 5 μL Annexin V-FITC and 5 μL PI (Propidium Iodide) and incubated in the dark at 37 $^{\circ}\text{C}$ for 20 min. After the described double staining, a total of 10,000 events per sample were acquired and fluorescence data were recorded and analyzed with a FACS Calibur flow cytometer accordingly.

2.6. Cell cycle and mitosis distribution detected by flow cytometry

A549 and 95D cells were collected and washed twice with ice-cold PBS after treated with YW3-56 (5, 10, 15 μM) for 48 h. Cells were then fixed with 70% ethanol overnight at -20°C . Cells were stained in solution with PI and RNase according to the manufacturer's instruction after twice washed with PBS. After staining, total of 20,000 cells per sample were acquired by using imaging flow cytometry (ImageStreamX Mk II instrument, Luminex, Seattle, USA), and cell cycle and mitosis distribution were analyzed accordingly.

2.7. Transcriptome sequencing and data analysis

A549 cells were treated with YW3-56 (0, 10 μM) for 48 h, and the mRNA was extracted with QIAGEN RNeasy kit (Germany, 74104). The samples were then sent to Novogene for quality inspection using Bioanalyzer 2100 system (Technologies, CA, USA). After qualified, the transcriptomes were sequenced and analyzed. Heatmaps and volcano maps were analyzed using the sangerbox (sangerbox.com) mapping website. KEGG analysis: KEGG and GSEA were analyzed on the online database OmicShare (omicshare.com). PPI network maps were analyzed using cytoscape software and MCODE app.

2.8. Statistical analysis

The bio-assay results were analyzed using Microsoft Excel 2021, and data were expressed as means \pm standard deviation (SD). At least three samples were prepared for each represented assay. Data analysis was performed using an ANOVA test. A P-value less than 0.05 was considered as statistically significant.

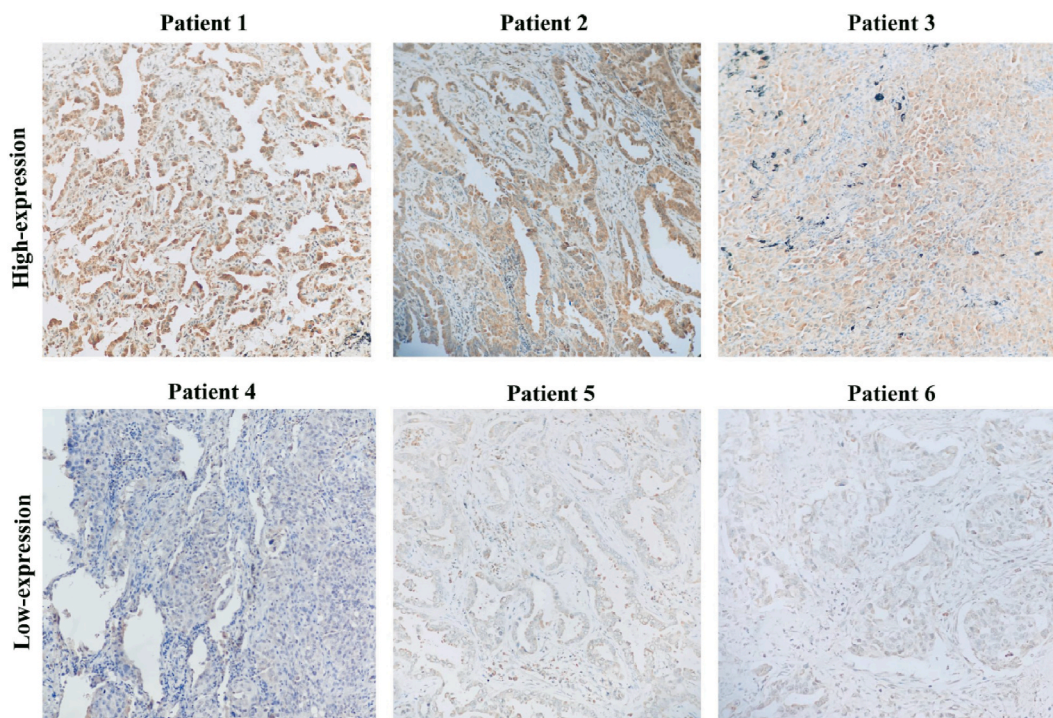


Fig. 1. Example of PAD4 high-expression and PAD4 low-expression in lung adenocarcinoma.

3. Results

3.1. Expression of PAD4 in lung adenocarcinoma

As we displayed in Fig. 1, the positive expression of PAD4 was located in the nucleus and cytoplasm. The total of 63 lung adenocarcinoma cases were divided into PAD4 high-expression group (23/63, 36.5%) and PAD4 low-expression group (40/63, 63.5%).

3.2. Correlation between PAD4 expression and clinicopathological characters

Statistical analysis showed that the high-expression rate of PAD4 were respectively 27.7% (13/47), 62.5% (10/16) in tissues of moderate - high differentiated and poor differentiated lung adenocarcinoma ($p < 0.05$). High-expression rate of PAD4 were 61.5% (8/13), 60.0% (9/15) in lung adenocarcinoma with lymphnode metastasis and pleural invasion, respectively, which obviously higher than patients without lymphnode metastasis and pleural invasion, and the difference was significant ($P < 0.05$). Positive expression rate of PAD4 was not significantly correlated with sexual distinction, patient age, tumor size and vascular cancer embolus ($p > 0.05$) (Table 1).

3.3. PAD4 inhibition decreased cell viability and induced apoptosis in lung cancer cell lines

To determine the effect of PAD4 inhibition in lung cancer cells, we used a previously reported PAD4 inhibitor, named YW3-56 as chemical structure was showed in Fig. 2A. YW3-56 demonstrates lung cancer cell growth inhibition activity in a concentration dependent manner as shown in Fig. 2B. A549 and 95D cells that treated with different concentration of YW3-56 were observed with decreased cell number as shown in Fig. 2C. We also used flow cytometry to detect of apoptosis induced by PAD4 inhibition in A549 and 95D cells as showed in Fig. 2D and E. The results indicated that PAD4 inhibition by YW3-56 could significantly enhance the frequency of apoptotic cell death.

3.4. RNA-sequencing analysis on PAD4 inhibitor on A549 lung cancer cells

In order to explore the mechanism of PAD4 inhibition by YW3-56 (10 μ M, 48 h) on A549 lung cancer cells, transcriptome sequencing was performed then. First, we analyzed the differential genes (DEGs) of the two sets of data (Control vs YW3-56), and the results showed that after YW3-56 treatment, the mRNA expression had a significant hierarchical clustering (Fig. 3A). Further screening of differential genes ($\text{padj} < 0.01$, $|\log_2\text{FoldChange}| \geq 2$), we found a total of 1520 differential genes including 784 up-regulated genes and 736 down-regulated genes (Fig. 3B). In this study, KEGG enrichment analysis of these differential genes was performed, and the results indicated that YW3-56 treatment affected mostly on the cell cycle, DNA replication, Valine, leucine and isoleucine biosynthesis, p53 signaling pathway and other pathways (Fig. 3C and D). Further, we performed GESA analysis on the KEGG results and found that the top1 pathway (cell cycle) was significantly decreased (Fig. 3E). Finally, we analyzed the genes in the cell cycle related protein-protein interaction using Cytoscape software (Fig. 3F), and found that most of the genes was down-regulated by PAD4 inhibition,

Table 1

Correlation between PAD4 expression and clinicopathological characters.

Parameter (n)	PAD4 expression (n%)		χ^2	P
	High-expression	Low-expression		
Sex				
Male (24)	7 (29.2)	17 (70.8)	0.901	0.342
Female (39)	16 (41.0)	23 (59.0)		
Age				
≤ 60 (24)	8 (33.3)	16 (66.7)	0.169	0.681
> 60 (39)	15 (38.5)	24 (61.5)		
Tumor size				
≤ 3 cm (43)	16 (37.2)	27 (62.8)	0.029	0.865
> 3 cm (20)	7 (35.0)	13 (65.0)		
Node metastasis				
Positive (13)	8 (61.5)	5 (38.5)	4.427	0.035
Negative (50)	15 (30.0)	35 (70.0)		
Cancer embolus				
Positive (16)	8 (50.0)	8 (50.0)	1.684	0.194
Negative (47)	15 (31.9)	32 (68.1)		
Pleural invasion				
Positive (15)	9 (60.0)	6 (40.0)	4.687	0.030
Negative (48)	14 (29.2)	34 (70.8)		
Differentiation				
Moderate - high (47)	13 (27.7)	34 (72.3)	6.251	0.012
Poor (16)	10 (62.5)	6 (37.5)		

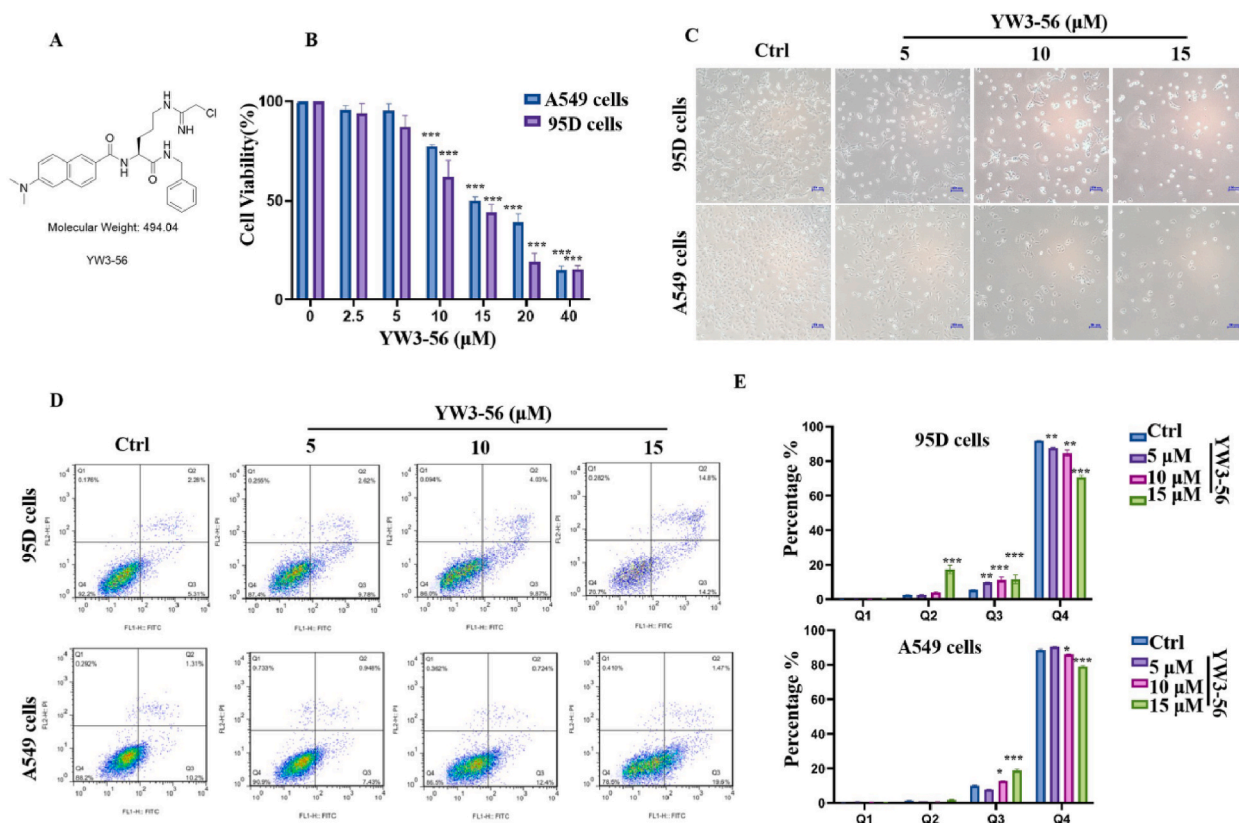


Fig. 2. PAD4 inhibitor YW3-56 against A549 and 95D lung cancer cells. A) Chemical structure of YW3-56. B) Cell Viability of A549 and 95D cells treated with different concentration of YW3-56 (0, 2.5, 5, 10, 15, 20, 40 μM) for 48 h. C) Cells images of A549 and 95D cells treated with different concentration of YW3-56. D) Flow cytometry analysis of apoptosis in A549 and 95D cells induced by different concentration of YW3-56. E) Apoptotic cell death in A549 and 95D cells induced by different concentration of YW3-56. Data shown were presented in bars as mean ± S.D. The statistical differences between the two groups were analyzed by two-sided unpaired Student's *t*-test. **p* < 0.0001 ***p* < 0.01, ****p* < 0.001 when compared with control; n = 3 independent samples per group.

including cell cycle process, mitotic cell cycle process. In conclusion, YW3-56 can significantly affect cell cycle, and mitotic cell cycle process-related genes.

3.5. PAD4 inhibition induced cell cycle and mitotic arrest in lung cancer cell lines

To further verify our discovery from RNA-sequencing analysis, we then detected cell cycle and mitosis distribution of A549 and 95D cells by flow cytometry. A549 and 95D cells were cultured with different concentration of YW3-56 (0, 5, 10, 15 μM) for 48 h. The results were displayed in Fig. 4A and B, based on our observation, PAD4 inhibition potent in accumulating cells in the G₁/G₀ phases and reducing the fraction of G₂/M and S phase cells. We then analyzed the mitosis process of A549 and 95D cells after PAD4 inhibition by YW3-56. Cells were imaged by MK II imaging flow cytometry using a 40× magnification and analyzed by IDEA 6.2. The dot plots as we showed in Fig. 5A displayed mitosis distribution, meanwhile, cell images in each mitosis phases were also showed as examples in Fig. 5B. Quantification of different phase of mitosis among different YW3-56 treatment groups as we displayed in Fig. 5C revealed that, telophase and prophase were increased by YW3-56 in a concentration-dependent manner. Frequency of prometa/metaphase cells (Pro/Meta) in A549 and 95D cells was increased by YW3-56, meanwhile, anaphase/telophase cells (Ana/Telo) was decreased. These observations demonstrate that PAD4 inhibition by YW3-56 could induce a mitotic arrest in lung cancer cells.

4. Discussion

PAD4 is a unique PAD isoenzyme and had been proven by multiple studies that it plays a key role in cancer progression and patients prognosis [16,17]. PAD4 could mediate neutrophil extracellular traps (NETs) formation, hence, promote immunosuppressive microenvironment in tumor [18,19]. Moreover, PAD4 expression was found higher in metastases than primary tumors [20]. In our study, PAD4 expression of 63 non-small cell lung cancer cases was observed, and our results indicated that PAD4 expression was higher in patients with lymphnode metastasis and pleural invasion (*P* < 0.05).

As a corepressor of p53 activity, PAD4 participates in inhibiting p53 transcriptional activity and regulating the expression of

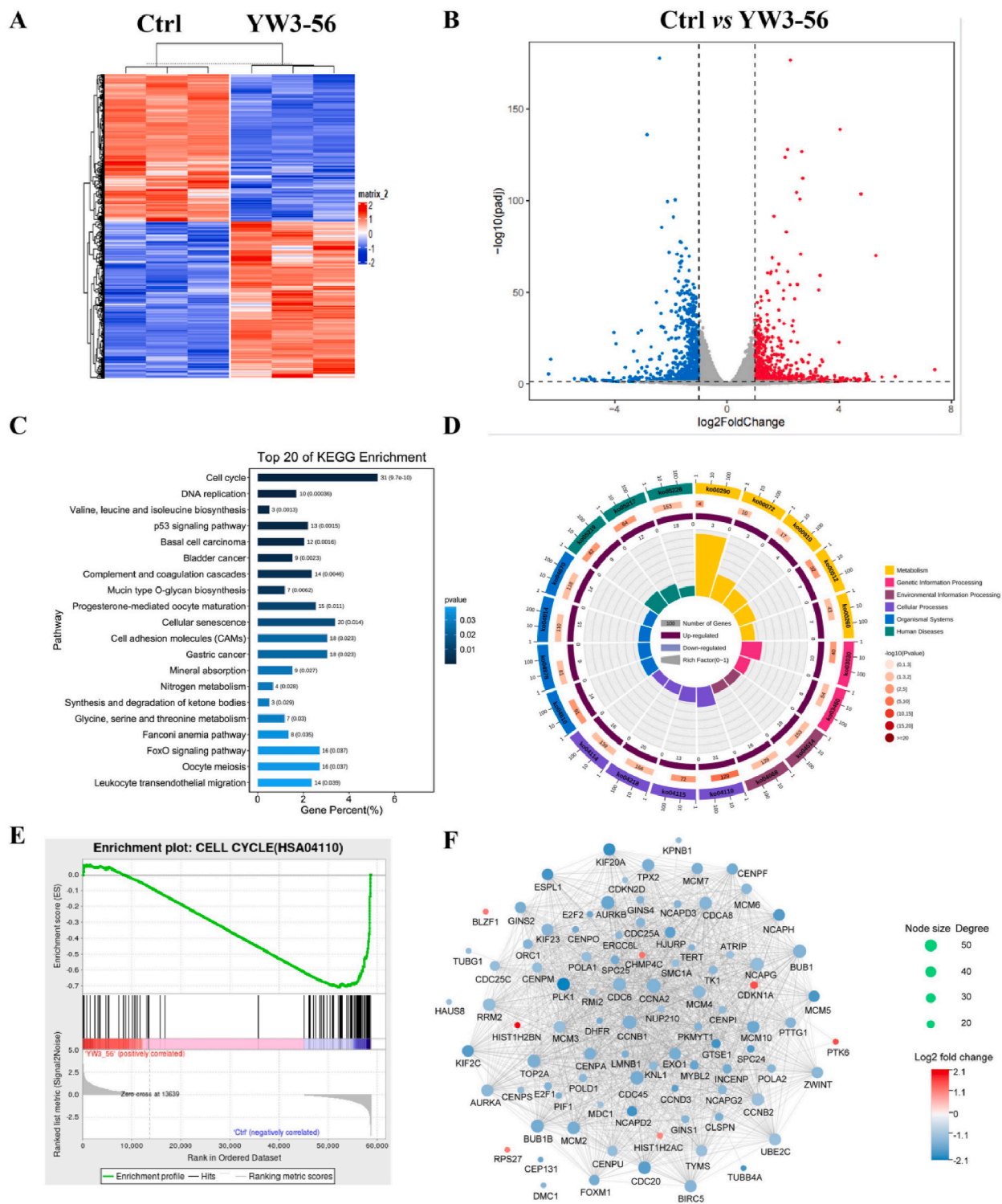


Fig. 3. Analysis of YW3-56 treatment induced transcriptomic differential in A549 cells. A) Hierarchical clustering results of differential gene expression after treatment of YW3-56 in A549 cells compared to control group. B) Volcano plot results of differential genes in A549 cells treated with YW3-56 compared to control group. C) The results of KEGG analysis revealed top 20 differential genes in A549 cell treated with YW3-56 compared to control group. D) KEGG analysis represented as enrichment circle plots revealed differential genes in A549 cells induced by YW3-56 treatment compared to control group. E) GSEA analysis results were performed on top1 (cell cycle) in the KEGG analysis results. F) Potential targets of YW3-56 treatment from PPI network analysis by Cytoscape software.

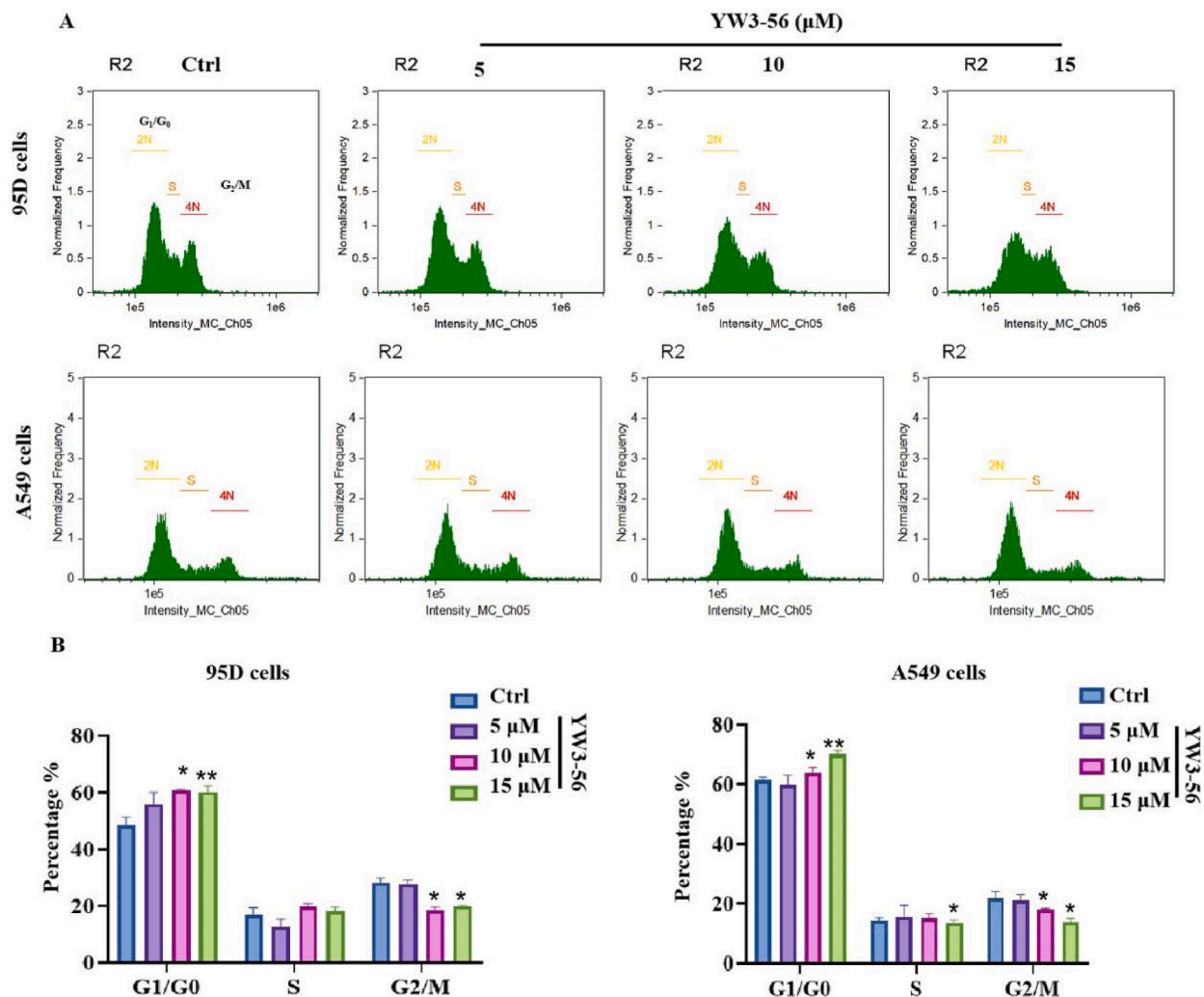


Fig. 4. PAD4 inhibitor YW3-56 induced cell cycle arrest in A549 and 95D lung cancer cells. A) Cell cycle distribution of A549 and 95D cells altered by different concentration of YW3-56. B) Treatment with YW3-56 in A549 and 95D cells induced increasing of G₁/G₀ phase, and decreasing of S phase. Data shown were presented in bars as mean \pm S.D. The statistical differences between the two groups were analyzed by two-sided unpaired Student's *t*-test. **p* < 0.0001 ***p* < 0.01, ****p* < 0.001 when compared with control; n = 3 independent samples per group.

multiple p53 target genes, indicating the important role it plays in regulating apoptosis. However, other studies suggest PAD4 to be transactivated by p53 via an intronic p53-binding site, allowing p53 to regulate protein citrullination. In their study, PAD4-knockout (KO) mice showed resistance to apoptotic stimulation and sustained decreased caspase-3 expression [21]. These results suggested that the role played by PAD4 in apoptosis could be cell type specific. In our study, a widely used PAD4 inhibitor, YW3-56 was administered on two non-small lung cancer cell lines. Our results indicated that the described lung cancer cells respond to YW3-56 treatment in a concentration dependent manner, with observation of cell morphology changes such as less attachment, rounding and shrinkage. We used RNA-sequencing to further investigate transcriptional changes that induced by PAD4 inhibition. Our results indicated that YW3-56 treatment affected mostly on the cell cycle, mitotic cell cycle process, p53 signaling pathway. In previous publication, PAD4 was proved promoting cell cycle [22], and involved in the repression of p53 target genes including p21/CIP1/WAF1 [23]. We then performed experiments to analyze cell cycle and mitosis in A549 and 95D cells with PAD4 inhibition. Based on our observation, PAD4 inhibited by YW3-56 could accumulate cells in the G₁/G₀ phases and reducing the fraction of G₂/M and S phase cells. Quantification of different phase of mitosis among different YW3-56 treatment groups revealed an increasing trend of telophase and prophase cells. Frequency of prometa/metaphase cells (Pro/Meta) was increased by PAD4 inhibition. These results demonstrated that PAD4 inhibition by YW3-56 in lung cancer cells could induce cell cycle and mitotic arrest. Those results were consistent with previous studies that performed on other types of tumor cells, such as osteosarcoma [14].

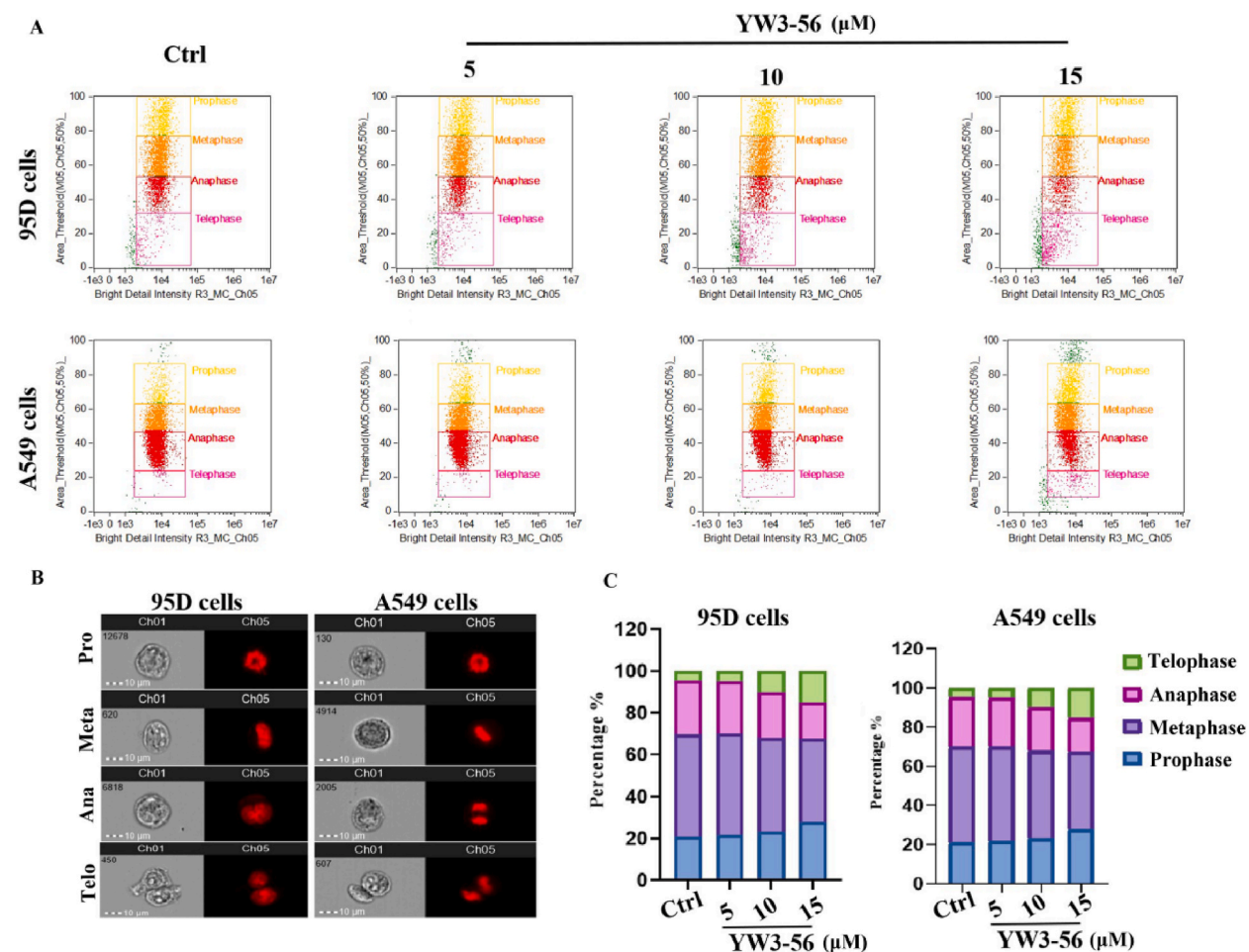


Fig. 5. PAD4 inhibitor YW3-56 induced mitosis arrest in A549 and 95D lung cancer cells. A) Distribution of mitosis in A549 and 95D cells altered by different concentration of YW3-56. B) Cells images of A549 and 95D cells treated with different concentration of YW3-56. C) Treatment with different concentration of YW3-56 for 48 h induces mitotic arrest in A549 and 95D cells. The statistical differences between the two groups were analyzed by two-sided unpaired Student's *t*-test. * $p < 0.0001$ ** $p < 0.01$, *** $p < 0.001$ when compared with control; $n = 3$ independent samples per group.

5. Conclusion

Taken together, our work suggest that PAD4 expression might contribute in metastasis in non-small lung cancer cells, and targeting PAD4 in NSCLC could induce a cell cycle and mitosis arrest. Also, our findings need to further expand the sample size in future research to substantiate.

Data availability statement

The experiment data used to support the findings of this study are available from the corresponding authors upon request.

CRediT authorship contribution statement

Xiangmei Wu: Writing – original draft, Methodology. **Liujia Chan:** Visualization, Software, Methodology. **Di Zhu:** Software. **Yuheng Pang:** Methodology. **Mulan Jin:** Conceptualization. **Yuji Wang:** Writing – original draft, Conceptualization. **Wenjing Wang:** Writing – original draft, Conceptualization.

Declaration of competing interest

The authors declare that they have no known competing financial interests or personal relationships that could have appeared to influence the work reported in this paper.

Acknowledgements

This work was supported by the Beijing Hospitals Authority Youth Programme (QML20192101, Xiangmei Wu), Beijing Municipal Colleges and Universities High Level Talents Introduction and Cultivate Project-Beijing Great Wall Scholar Program from Beijing Municipal Education Commission, grant number (CIT&TCD 20180332, Yuji Wang).

References

- [1] H. Sung, J. Ferlay, R.L. Siegel, M. Laversanne, I. Soerjomataram, A. Jemal, F. Bray, Global cancer statistics 2020: GLOBOCAN estimates of incidence and mortality worldwide for 36 cancers in 185 countries, *Ca - Cancer J. Clin.* 71 (2021) 209–249, <https://doi.org/10.3322/caac.21660>.
- [2] L. Succony, D.M. Rassl, A.P. Barker, F.M. McCaughan, R.C. Rintoul, Adenocarcinoma spectrum lesions of the lung: detection, pathology and treatment strategies, *Cancer Treat. Rev.* 99 (2021) 102237, <https://doi.org/10.1016/j.ctrv.2021.102237>.
- [3] J.A. Chen, J.W. Riess, Advances in targeting acquired resistance mechanisms to epidermal growth factor receptor tyrosine kinase inhibitors, *J. Thorac. Dis.* 12 (2020) 2859–2876, <https://doi.org/10.21037/jtd.2019.08.32>.
- [4] L. Osmani, F. Askin, E. Gabrielson, Q.K. Li, Current WHO guidelines and the critical role of immunohistochemical markers in the subclassification of non-small cell lung carcinoma (NSCLC): moving from targeted therapy to immunotherapy, *Semin. Cancer Biol.* 52 (2018) 103–109, <https://doi.org/10.1016/j.semcancer.2017.11.019>.
- [5] R.S. Herbst, D. Morgensztern, C. Boshoff, The biology and management of non-small cell lung cancer, *Nature* 553 (2018) 446–454, <https://doi.org/10.1038/nature25183>.
- [6] A. Bishayee, K. Block, A broad-spectrum integrative design for cancer prevention and therapy: the challenge ahead, *Semin. Cancer Biol.* 35 (Suppl) (2015) S1–S4, <https://doi.org/10.1016/j.semcancer.2015.08.002>.
- [7] S. Mondal, P.R. Thompson, Protein arginine deiminases (PADs): biochemistry and chemical biology of protein citrullination, *Acc. Chem. Res.* 52 (2019) 818–832, <https://doi.org/10.1021/acs.accounts.9b00024>.
- [8] Y. Zhang, Y. Yang, X. Hu, Z. Wang, L. Li, P. Chen, PADs in cancer: current and future, *Biochim. Biophys. Acta Rev. Canc* 1875 (2021) 188492, <https://doi.org/10.1016/j.bbcan.2020.188492>.
- [9] K. Nakashima, T. Hagiwara, A. Ishigami, S. Nagata, H. Asaga, M. Kuramoto, T. Senshu, M. Yamada, Molecular characterization of peptidylarginine deiminase in HL-60 cells induced by retinoic acid and 1 α ,25-dihydroxyvitamin D(3), *J. Biol. Chem.* 274 (1999) 27786–27792, <https://doi.org/10.1074/jbc.274.39.27786>.
- [10] B. Kolarz, M. Ciesla, M. Drygiewska, M. Majdan, Peptidyl arginine deiminase type 4 gene promoter hypo-methylation in rheumatoid arthritis, *J. Clin. Med.* 9 (2020), <https://doi.org/10.3390/jcm9072049>.
- [11] Y. Wang, R. Chen, Y. Gan, S. Ying, The roles of PAD2- and PAD4-mediated protein citrullination catalysis in cancers, *Int. J. Cancer* 148 (2021) 267–276, <https://doi.org/10.1002/ijc.33205>.
- [12] X. Chang, J. Han, L. Pang, Y. Zhao, Y. Yang, Z. Shen, Increased PAD4 expression in blood and tissues of patients with malignant tumors, *BMC Cancer* 9 (2009) 40, <https://doi.org/10.1186/1471-2407-9-40>.
- [13] M. Liu, Y. Qu, X. Teng, Y. Xing, D. Li, C. Li, L. Cai, PAD4-mediated epithelial-mesenchymal transition in lung cancer cells, *Mol. Med. Rep.* 19 (2019) 3087–3094, <https://doi.org/10.3892/mmr.2019.9968>.
- [14] Y. Wang, P. Li, S. Wang, J. Hu, X.A. Chen, J. Wu, M. Fisher, K. Oshaben, N. Zhao, Y. Gu, D. Wang, G. Chen, Y. Wang, Anticancer peptidylarginine deiminase (PAD) inhibitors regulate the autophagy flux and the mammalian target of rapamycin complex 1 activity, *J. Biol. Chem.* 287 (2012) 25941–25953, <https://doi.org/10.1074/jbc.M112.375725>.
- [15] L. Chan, Y. Pang, Y. Wang, D. Zhu, A. Taledaohan, Y. Jia, L. Zhao, W. Wang, Genistein-induced mitochondrial dysfunction and FOXO3a/PUMA expression in non-small lung cancer cells, *Pharm. Biol.* 60 (2022) 1876–1883, <https://doi.org/10.1080/13880209.2022.2123933>.
- [16] X. Wu, Y. Wang, W. Wang, The role of peptidyl arginine deiminase IV(PAD4) in cancers, *Anti Cancer Agents Med. Chem.* 23 (2022) 256–265, <https://doi.org/10.2174/1871520622666220614115309>.
- [17] D. Zhu, Y. Lu, Y. Wang, Y. Wang, PAD4 and its inhibitors in cancer progression and prognosis, *Pharmaceutics* 14 (2022), <https://doi.org/10.3390/pharmaceutics14112414>.
- [18] D. Zhu, Y. Lu, L. Gui, W. Wang, X. Hu, S. Chen, Y. Wang, Y. Wang, Self-assembling, pH-responsive nanoflowers for inhibiting PAD4 and neutrophil extracellular trap formation and improving the tumor immune microenvironment, *Acta Pharm. Sin.* B 12 (2022) 2592–2608, <https://doi.org/10.1016/j.apsb.2021.11.006>.
- [19] H. Wang, H. Zhang, Y. Wang, Z.J. Brown, Y. Xia, Z. Huang, C. Shen, Z. Hu, J. Beane, E.A. Ansa-Addo, H. Huang, D. Tian, A. Tsung, Regulatory T-cell and neutrophil extracellular trap interaction contributes to carcinogenesis in non-alcoholic steatohepatitis, *J. Hepatol.* 75 (2021) 1271–1283, <https://doi.org/10.1016/j.jhep.2021.07.032>.
- [20] A.E. Yuzhalin, A.N. Gordon-Weeks, M.L. Tognoli, K. Jones, B. Markelc, R. Konietzny, R. Fischer, A. Muth, E. O'Neill, P.R. Thompson, P.J. Venables, B.M. Kessler, S.Y. Lim, R.J. Muschel, Colorectal cancer liver metastatic growth depends on PAD4-driven citrullination of the extracellular matrix, *Nat. Commun.* 9 (2018) 4783, <https://doi.org/10.1038/s41467-018-07306-7>.
- [21] C. Tanikawa, M. Espinosa, A. Suzuki, K. Masuda, K. Yamamoto, E. Tsuchiya, K. Ueda, Y. Daigo, Y. Nakamura, K. Matsuda, Regulation of histone modification and chromatin structure by the p53-PAD4 pathway, *Nat. Commun.* 3 (2012) 676, <https://doi.org/10.1038/ncomms1676>.
- [22] H. Chen, L. Wei, M. Luo, X. Wang, Y. Zhan, Y. Mao, C. Huang, J. Li, H. Lu, PAD4 inhibitor promotes DNA damage and radiosensitivity of nasopharyngeal carcinoma cells, *Environ. Toxicol.* 36 (2021) 2291–2301, <https://doi.org/10.1002/tox.23342>.
- [23] P. Li, H. Yao, Z. Zhang, M. Li, Y. Luo, P.R. Thompson, D.S. Gilmour, Y. Wang, Regulation of p53 target gene expression by peptidylarginine deiminase 4, *Mol. Cell Biol.* 28 (2008) 4745–4758, <https://doi.org/10.1128/MCB.01747-07>.